



# Evaluating the implementation of shallow water equations within numerical models focusing the propagation of dambreak waves

R. Liem, J. Schramm & J. Köngeter

*Institute of Hydraulic Engineering and Water Resources Management (IWW), Aachen, Germany*

## Abstract

Specifically flow conditions during the initial stage of a dambreak wave differ from shallow water equations (*SWE*), which are usually applied as the basic physical equations in numerical simulations on dambreak waves. To quantify the deviation of shallow water equations from the actual dambreak wave's propagation, experiments are conducted using a High-Speed-Measuring-System providing frequencies up to 4500 frames/sec. In particular front positions and front velocities are observed from the digital recordings. Since it has been shown that varying numerical methods can cause different computational results, numerical test series have also been carried out considering a finite element and a finite volume approach as well as different resolutions in time and space. Comparison of numerical and experimental results, in particular front velocities, underline that shallow water equations have to be adapted towards a more accurate physical approach.

## 1 Introduction

During the last decade 1D- as well as 2D-depth averaged computations of dam break waves, based on *SWE*, have become a common tool to predict propagation times and water levels for the development of emergency action plans in case of a failure.

Even though numerical methods themselves have been improved increasingly, test cases, which were computed by several numerical modellers, have lead to different results, in particular concerning the propagation times of a



## 232 Computational Methods and Experimental Measures

dambreak wave [1]. Besides there has been rather less effort on focusing the physical applicability of shallow water theory to dambreak waves. In particular flow conditions within the initial stage right after a dam-failure are strongly influenced by vertical flow phenomena, which are totally neglected within shallow water equations. Therefore, the entire computation of a dambreak wave might not only be influenced by varying numerical methods but by the lack of knowledge about hydrodynamic processes, which causes the evaluation of inaccurate propagation times of the flood wave. Taking into consideration that calibration of numerical models for cases of catastrophes is not possible, the deviation of the physical equations compared to real flow conditions becomes even more meaningful.

## 2 Application of shallow water theory

### 2.1 Basic equations

To derive *SWE* from three-dimensional *Navier-Stokes-equations* flow conditions within a free surface flow have to meet the assumptions of *shallow water theory*. In particular vertical flow phenomena in comparison to horizontal flow as well as vertical movement of the free surface have to be negligible. Also the approximation of hydrostatic pressure has to be applicable, which is only valid if vertical acceleration does not exist. For one-dimensional flow *SWE* can be denoted as follows:

$$\frac{\partial h}{\partial t} + \frac{\partial(uh)}{\partial x} = 0 \quad (1)$$

$$\frac{\partial u}{\partial t} + u \frac{\partial u}{\partial x} = -g \frac{\partial h}{\partial x} \quad (2)$$

considering  $h$  as water depth,  $u$  as flow velocity in  $x$ -direction and  $g$  as acceleration due to gravity. The equations are denoted as they are used later on within numerical simulation of the experiments, neglecting any source and sink term, as induced by friction losses and bed slopes.

### 2.2 Ritter's dambreak wave solution

*Ritter* in 1892 has been the first to investigate on dam break problems analytically [2]. His results are mentioned very frequently in literature and have been used quite often for comparison of experimental and numerical data. Based on shallow water theory he derived the velocity of the positive front wave as

$$u_F = 2\sqrt{g \cdot H_0} \quad (3)$$

where  $H_0$  is the initial height of the reservoir.

Evidently *Stoker* applied the method of characteristics to one-dimensional SWE and derived the same front velocity for dambreak waves on dry frictionless horizontal beds as found by *Ritter* [3]. It has to be noticed that the given equation represents a constant front velocity, presuming a quasi-steady behaviour of the dambreak wave, even though water masses at the beginning are strongly accelerated from motionlessness.

*Ritter's* analytical solution has not only been used as verification test case for numerical models but as initial condition within certain numerical methods (s. [4] and [5]). Numerical models considering *Ritter's* solution as initial condition will lead to the above solution itself, if test conditions correspond to certain conditions as found in the experiment, which is introduced in section 3. Therefore this kind of numerical model is excepted from the numerical tests in section 4, since comparison to experimental data can be carried out by considering *Ritter's* solution itself.

## 2.3 Modelling scale

As found in common literature front positions  $x_F$ , front velocities  $u_F$  and propagation times  $t$  can be put on a uniform dimensionless scale by using the following equations (s. e.g. [6]):

Table 1: Dimensionless notation of dambreak wave parameters

$x_F$	$u_F$	$t$
$X_F = \frac{x_F}{H_0}$	$U_F = \frac{u_F}{\sqrt{g \cdot H_0}}$	$T = t \cdot \sqrt{\frac{g}{H_0}}$

These equations are actually based on the applicability of *Froude's* law and will be used for later evaluation and comparison of experimental and numerical data.

## 2.4 Former research on dambreak waves

SWE have widely been used for numerical modelling of dambreak waves. Besides different techniques in CFD such as finite-differences, finite-volumes or finite-elements methods, several numerical algorithms exist to solve SWE due to instability, initiated by free surface flow among initially dry beds and by intense source and sink terms, such as friction losses or bed slopes (e.g. [4] and [5]). As a consequence different numerical models can cause different results focusing the same test case. Recent investigations on numerical modelling as carried out by [1] suggested that the speed of a dambreak wave and therefore its propagation time is often poorly predicted. Modelling tests based on laboratory test cases and the real failure of Malpasset indicated that 1D-models overestimate and 2D-models underestimate front velocities. Reasons for this might not only be numerical methods themselves but differences in mesh size and time resolution.

## 234 Computational Methods and Experimental Measures

The authors of [7] and [8] have been known for carrying out recent experiments on dam break waves using digital image processing providing frequencies of 25 to 50 frames per second. According to [7] a dam break wave can be divided into an initial wave and a dynamic wave, which is passing the initial wave at a defined location  $x$ . In [8] water levels acquired from the recorded frames indicated, that Stoker's solution, Ritter's respectively applies as soon as a stable wave front has been shaped from a rather jet-shaped wave front.

Besides these investigations there has been hardly any experimental work on dam break waves in smooth horizontal channels even though there is still a lack of knowledge concerning flow conditions within the positive wave front in particular during the initial stage. This might be caused by the high demand on measuring technique which has to be provided for extremely unsteady and speedy flow.

### 3 Experiments on dambreak

#### 3.1 Experimental set up

##### 3.1.1 Dambreak wave channel

A linear rectangular channel of 14 m length and 0.50 m width has been set up for dam break experiments (s. Figure 1). Since the construction of the whole channel as well as its bottom is made of steel, windows of 20x20 cm had to be cut to enable optical measuring techniques (s. next section). The bottom is covered by glass to ensure a smooth bottom.

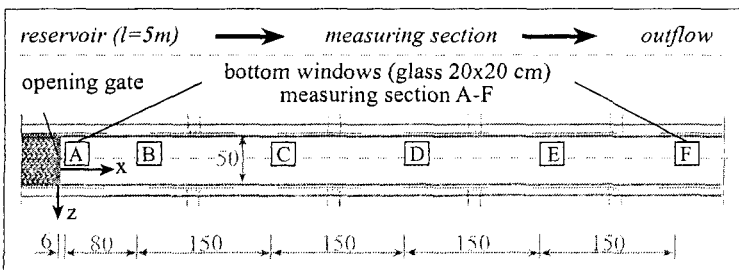


Figure 1: Top view of the dambreak wave channel

The functionality of the opening mechanism had to be observed very thoroughly, since different shapes of the wave front as found in literature might be caused by the movement and the acceleration of the opening gate. Ideal conditions will be met, if a vertical free standing water plane corresponding to initial conditions within mathematical approaches are established. Since an upward or downward movement will cause water to run off above or underneath the opening gate before it is entirely opened a forward movement would be an optimum. Unfortunately there seems to be no reasonable frictionless solution of

using a forward moving gate during an experiment. Therefore a combination of a forward and upward movement has been chosen, which is initiated by a high-speed pneumatic system. In this way a vertical water plane was established within less than  $5/100$  of a second.

### 3.1.2 Measuring techniques

A high-speed camera providing frequencies up to 4500 Hz is used to acquire digital recordings of the dambreak wave. Compared to usual cameras a very low spatial resolution of  $256 \times 256$  pixels and very short exposure times due to high frequencies are provided. Therefore the maintenance of a minimum recording quality requires a strong light source for water illumination.

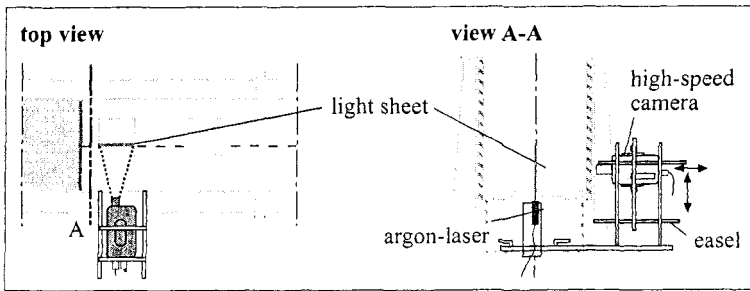


Figure 2: Set up of the measuring equipment

To observe flow behaviour within a vertical plane a light sheet is projected by an Argon-laser of 300 Watt through the bottom as sketched in Figure 2. Due to extremely moving water levels and induced air reflections have to be filtered by additional optical filters, which have to be mounted to the camera objective.

### 3.2 Test series and data analysis

Experiments were conducted considering four different initial water depths,  $H_0 = 30, 35, 40$  and  $45$  cm, within the reservoir to verify the applicability of modelling scales. An experiment for one initial water depth includes six recordings of the dambreak wave at each measuring section (s. Figure 1) of the channel. In this way 144 recordings, each consisting of 200 to 300 frames, were taken and analysed. The front position  $x_F$  of the dambreak wave can be scanned directly from the recorded frames by analysing the greyscale distribution. Standard deviations of the obtained front positions were ranging between 0.7 and 1.6 mm depending on the initial water depth and the investigated measuring section.

In consideration of variance propagation by means of statistics front velocities were derived from every two front positions with a time distance of  $dt = 0.01$  s in between. In this way the standard deviation of the derived front velocities was limited to a maximum of 3 % of the average front velocities.

### 3.3 Experimental results

In Figure 3 mean values of front positions  $x_F$  versus propagation time  $t$  are plotted for every investigated  $H_0$ . Of course measuring data was only obtained within the marked rectangles. Lines only represent a trend, derived from the gradients of the measuring data, which belongs to each section.

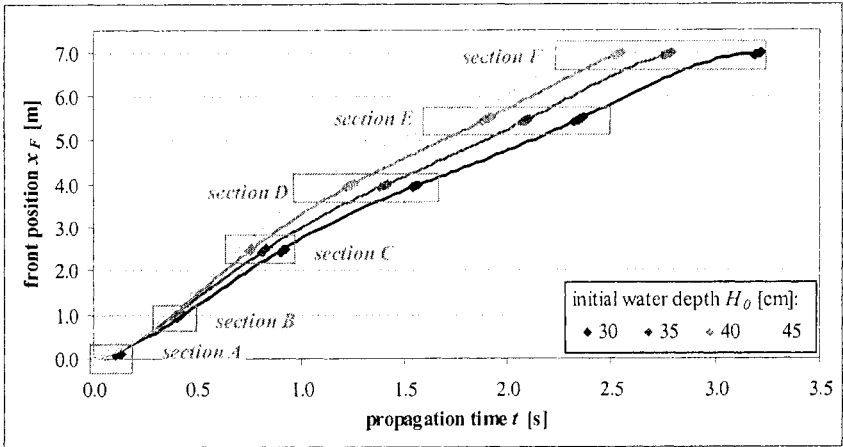


Figure 3: Resulting front positions  $x_F$  versus propagation time  $t$

It can be noticed that scaling, as it is introduced earlier, might be applicable to the measuring data due to the similar progression of the curves. Anyway, since propagation times and front positions of a dambreak wave always follow a steady rising curve, plotting and analysing front positions versus time itself is not very meaningful. Eventually velocities and acceleration processes have significant influence on the propagation of the dambreak wave. Therefore in Figure 4 derived front velocities versus propagation time are plotted.

Again actual data is only available among the measuring sections. Data belonging to one section has been separated by dashed lines. Curves as before indicate the trend of data, which indicates similarity between experiments based on different scales. In particular a significant rise and fall can be noticed within the first second. Afterwards smoother fluctuation than during the initial stage, can be presumed, since more sophisticated interpretation has to be undertaken by using a dimensionless scale as it is done within the final evaluation in section 5.

Also from this figure a strong fluctuation of velocities can be noticed, which indicates the strong influence of turbulent flow conditions within the dambreak wave. Due to the lack of data between the measuring sections it has been quite complex to separate unsteady behaviour from turbulence and error propagation. Therefore in section 5 only time averaged velocities will be used for further comparison.

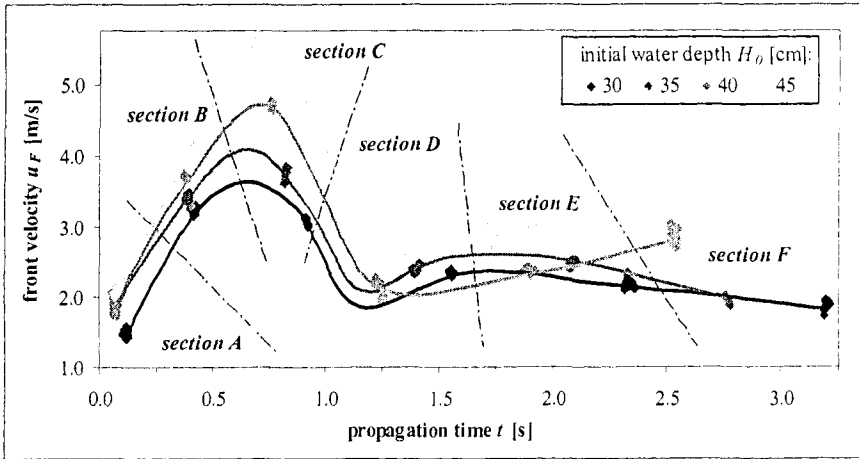


Figure 4: Resulting front velocities  $u_F$  versus propagation time  $t$

## 4 Numerical modelling

### 4.1 Numerical test series

To simulate the described laboratory tests a finite element as well as a finite volume approach implementing *SWE* has been chosen for 1D modelling. The finite element model (FEM) is based on *Rismo* as described in [9], which has mainly been used for river modelling. The model does not provide any front capturing method. FE-dambreak simulations are carried out using an implicit scheme. Finite volume modelling (FVM) is conducted using *Fluvius*, which has also been developed for 1D-river modelling [10]. Front capturing is done using high resolution techniques within an explicit scheme, whereby a adaptive time resolution towards fixed *Courant* numbers can be chosen. For further information about the applied models the denoted literature shall be reviewed.

Several test series were conducted not only considering different initial water depths as investigated in the experiments but also differing in space and time resolution:

Table 2: Time spacing and element sizes for numerical modelling

	FEM			FVM		
	$dt$ [s]			$Cu$ [-]		
$dx$ [m]	0.0050	0.0010	0.0005	1.0	0.9	0.5
0.002	x	x	x	x	x	x
0.005	x	x	x	x	x	x
0.010	x	x	x	x	x	x
0.020				x	x	x

238 *Computational Methods and Experimental Measures*

Since each test was carried out for four initial water depths 36 FEM and 32 FVM based simulations were carried out.

#### 4.2 Modelling performance

The performance of the numerical models can be observed in Figure 5 and Figure 6. Observing the average front velocities based on a dimensionless scale resulting from FEM based simulation, average Courant numbers can be derived as well, varying between 0.1 and 10.

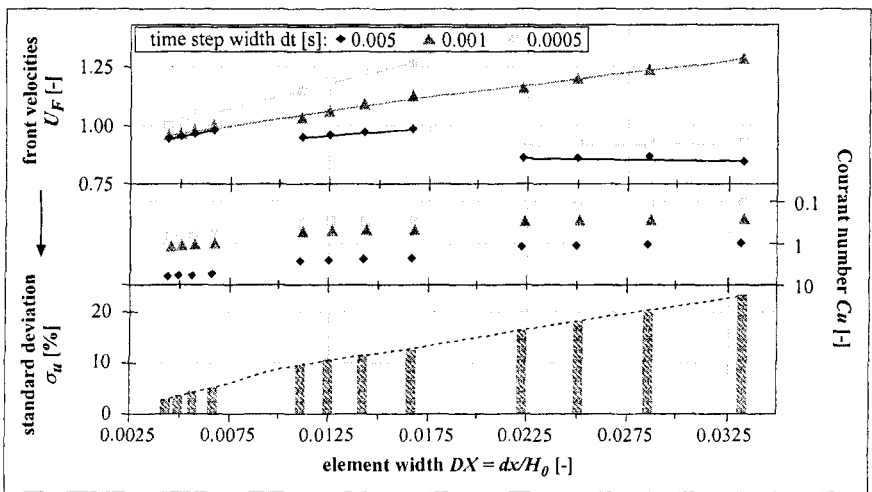


Figure 5: Performance of FEM on dambreak simulation

As can be seen velocity variation is rather depending on mesh size than on time spacing. Standard deviation of the average front velocities  $\sigma_u$  derived for different time steps decreases with decreasing dimensionless element size  $DX$ . In consideration of a maximum acceptable  $\sigma_u$  it is possible to specify an element size  $dx$  depending on the initial water depth  $H_0$  within the reservoir, which is required to do valid FEM based dambreak simulation at least close to the dam site, where steepest velocity gradients are expected.

In comparison FVM based results are varying within a much smaller range, neglecting test series with a Courant number of 0.5, which do not meet a reasonable velocity range and are therefore neglected within the following graph. Standard deviations of the average front velocities regarding absolute element sizes  $dx$  are smaller respectively and do not indicate a certain trend as found before. Since standard deviations for  $Cu = 1.0$  are less than for  $Cu = 0.9$ , the choice of  $Cu = 1.0$  has to be recommended due to its higher effectiveness concerning computation times. Overall front velocities resulting from both numerical approaches are quite identical.



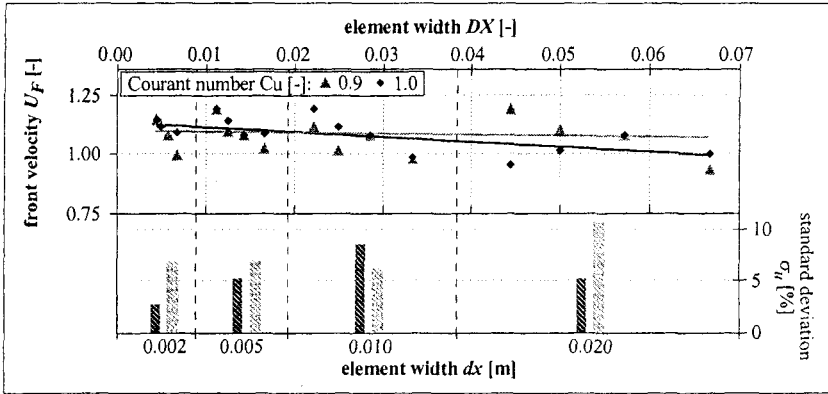


Figure 6: Performance of FVM on dambreak simulation

## 5 Final evaluation

Final comparison of dimensionless front velocities  $U_F$  is presented in Figure 7. While experimental data is significantly fluctuating, numerical data is staying at a constant level which is reached immediately after the initial time step. The value of numerically obtained front velocities depends on the entire numerical set up as described earlier.

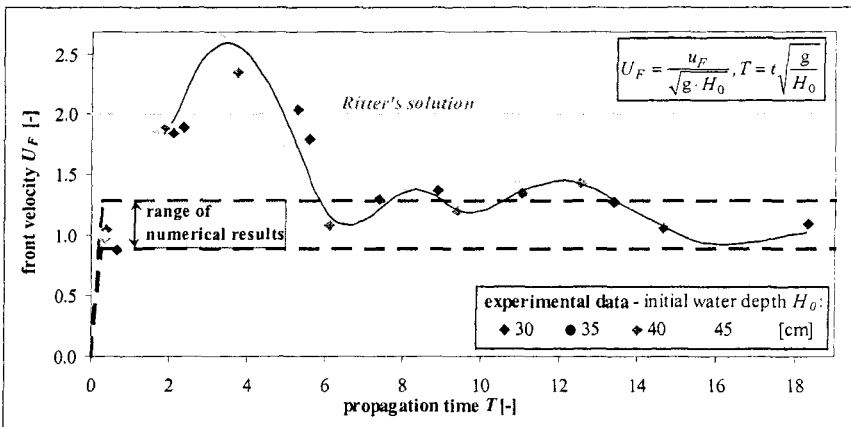


Figure 7: Comparison between experimental and numerical data

Focusing experimental data the initial stage depending on its definition seems to last much longer than found in common literature (s. e.g. [2] or [6]) where values of the initial time  $T_i$  range between 0,7 and 1,4. Assuming that the first

steep increase and decrease of  $U_F$  belong to the initial stage  $T_i$  equals rather 6. In addition maximum experimental data is exceeding the range of numerical data as well as Ritter's solution, even though experimental data approaches numerical data at a later stage.

## 6 Conclusions and future research

It has been proven, that vertical flow phenomena during the initial stage of a dambreak wave are too significant to be neglected as it is done by *shallow water theory*. Since front velocities within the initial stage resulting from numerical simulation based on *SWE* are lower than actually found by detailed measurements, propagation times not only within the initial stage but also at a later point of time are over estimated because of the propagating error.

While numerical methods are quite stable against variances and can be limited by using reasonable mesh sizes, the implemented equations themselves need to be improved. This can be done by considering an additional time dependent source term within the basic equations, which has to be derived from experimental data. A more sophisticated approach to optimise *SWE* can be established by detailed measurements of the velocity field within the dambreak wave, which are currently carried out by particle-image-velocimetry (PIV).

## 7 References

- [1] CADAM (2000): "Concerted Action on Dambreak Modelling – Final Report", ENV4-CT97-0555, SR 571
- [2] Ritter, A. (1892): "Die Fortpflanzung der Wasserwellen", Zeitschr. des VDI" 1892, 947 – 954
- [3] Stoker, J. J. (1957): "Water Waves - The Mathematical Theory with Applications", New York
- [4] Fraccorollo, L.; E.F. Toro (1995): "Experimental and numerical assessment of the shallow water model for two-dimensional dam-break type problems", J. Hydr. Res., 33, 843 -863
- [5] Nujic M. (1995): "Efficient implementation of non-oscillatory schemes for the computation of free-surface flows", J. Hydraulic Res., 33(1), 101 - 111
- [6] Martin, H. (1970): "Entleerungsströmungen in unterschiedlich geformten Staubecken", Diss., Univ. Dresden
- [7] Lauber G.; W. H. Hager (1998): "Experiments to dam break wave: Horizontal channel", J. Hydraulic Res., 36, 291 – 307
- [8] Stansby , P.K.; A. Chegini; T. C. D. Barnes (1998): „The initial stages of dambreak flow”, J. Fluid Mech., Cambridge University Press, 374, 407-424
- [9] Rouvé, G.; M. Schröder (1994): "Die Entwicklung eines mathematisch-numerischen Verfahrens zur Berechnung naturnaher Fließgewässer"; DFG Ro-365/31-6
- [10] Schramm, J; S. Enk, J. Köngeter (1999): „One-dimensional calculation of unsteady compound open channel flow using adaptive mesh refinement”, Int. Conf.: Godunov Methods - Theory and Applications, Oxford, UK